Electrochemical characterization of the artificial metalloenzyme papain-[(η6-arene)Ru(1,10-phenanthroline)Cl]+

Štěpánka Nováková Lachmanová, Lubomír Pospíšil, Jakub Šebera, Barisa Talbi, Michèle Salmain, Magdaléna Hromadová

Electrochemical characterization of the artificial metalloenzyme papain-[(η^6-arene)Ru(1,10-phenanthroline)Cl]$^+$.

Štěpánka Nováková Lachmanová[a], Lubomír Pospíšil[a], Jakub Šebera[a], Barisa Talbi[b], Michèle Salmain[b], Magdaléna Hromadová[a,*]

[a] *J. Heyrovský Institute of Physical Chemistry of the CAS, v.v.i., Dolejškova 3, 18223 Prague, Czech Republic*

[b] *Sorbonne Université, CNRS, Institut Parisien de Chimie Moléculaire (IPCM), 4 place Jussieu, F-75005 Paris, France*

Keywords: artificial metalloenzyme; papain; electrochemical admittance and impedance techniques; ruthenium(II) complexes;

Abstract

Electrochemical properties were studied for [(η^6-arene)Ru(1,10-phenanthroline)Cl]Cl (arene = $C_6H_5(CH_2)_2NHCOCH_2Cl$) organometallic complex **1**, protein Papain **PAP** and its conjugate with organometallic complex **1-PAP**. The latter can serve as an artificial metalloenzyme with catalytic activity in transfer hydrogenation. This work demonstrates that AC voltammetry and electrochemical impedance spectroscopy can be used as fast tools to screen the catalytic ability of **1-PAP** electrochemically by studies of the catalytic hydrogen evolution reaction (HER). Proteins are known to catalyze this process, but we have shown that additional HER signal associated with the catalytic activity of **1** is observed for its conjugate with Papain **1-PAP**.

* Corresponding author: hromadom@jh-inst.cas.cz

1. Introduction

The aim of this paper is to characterize electrochemically an artificial metalloenzyme **1-PAP** (see Scheme 1) prepared by covalent coupling between the [(η^6-arene)Ru(1,10-phenanthroline)Cl]Cl (arene = $C_6H_5(CH_2)_2NHCOCH_2Cl$) complex **1** and the sulfhydryl group of the sole free cysteine Cys25 in the active site of the endoproteinase Papain (EC 3.4.22.2) **PAP** from *Carica papaya* [1]. Focus will be on the catalytic hydrogen evolution reaction (HER) in the presence of free organometallic complex **1**, free protein **PAP** and its bioconjugate **1-PAP**. Such reaction can serve as a fast tool for elucidation of the catalytic ability of the artificial metalloenzyme towards transfer hydrogenation reactions.

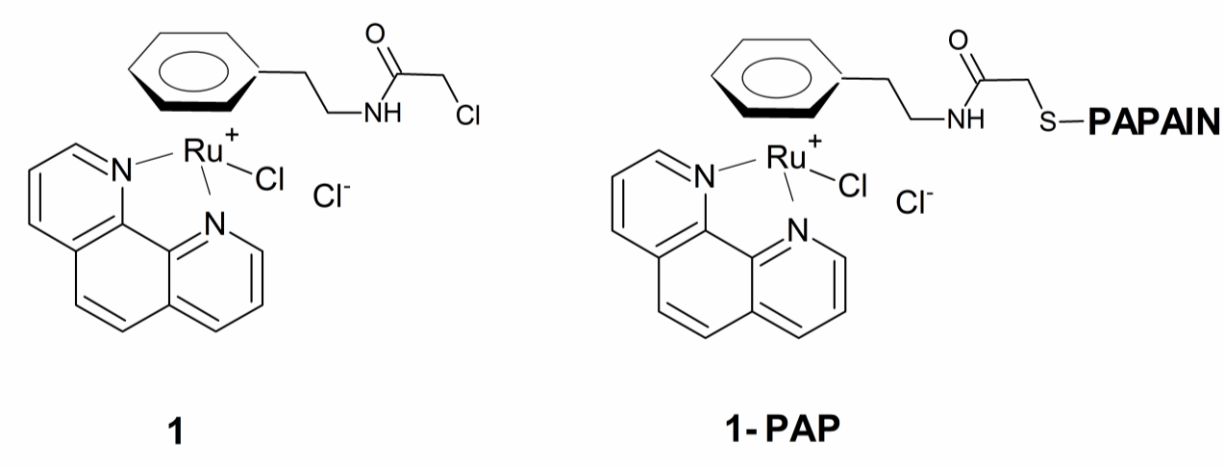

Chart 1. Chemical structures of compound **1** and its conjugate with papain **1-PAP**.

1.1. Electrochemical properties of Ru(II) complexes

Electrochemical properties of Ru(II) complexes have been reviewed by Ghosh and Chakravorty [2]. The simplest complex related to this study is $[Ru(phen)_3]^{2+}$ (phen = 1,10-phenanthroline). It can be oxidized to $[Ru(phen)_3]^{3+}$ and each coordinated ligand can be reduced reversibly by acceptance of one electron [3]. Further ligand reduction at more negative potentials is also possible [4]. In an ideal case, two sets of three one–electron transfers should be possible, i.e. transfer of two electrons per each ligand. Indeed, free phen

displays two quasi-reversible one-electron reductions in cyclic voltammetry [5] observed at more negative potentials compared to the coordinated ligands in the $[Ru(phen)_3]^{3+}$ complex.

In the context of this work the most important Ru(II) complexes studied so far are $[(arene)M(phen)Cl]^+$ complexes, where arene = η^5-C_5Me_5 or η^6-C_6Me_6, M = Rh, Ir, Ru. They were studied electrochemically as potential transfer hydrogenation catalysts [6]. The authors showed that the first reduction step in acetonitrile involves transfer of two electrons and explained it by a reductive removal of the chloride ligand according to

$$[(\eta^5\text{-}C_5Me_5)M(phen)Cl]^+ + 2e^- \longrightarrow [(\eta^5\text{-}C_5Me_5)M(phen)] + Cl^- \qquad [1]$$

Authors also postulated that the electrogenerated neutral species is not stable and thus stated that the exact nature of this redox process remains still unclear.

Štěpnička *et al.* [7] further studied the electrochemical properties of cationic complexes $[(\eta^6\text{-arene})Ru(phen)Cl]^+$ (arene = C_6H_6 or C_6Me_6) in acetonitrile in order to rationalize the transfer hydrogenation catalytic activity of their respective aqua complexes $[(\eta^6\text{-arene})Ru(phen)(OH_2)]^{2+}$ that could not be studied directly due to their instability. The $[(\eta^6\text{-arene})Ru(phen)Cl]^+$ species can be viewed as precursors of such catalytically active aqua complexes in water environment. The first reduction step of $[(\eta^6\text{-arene})Ru(phen)Cl]^+$ complexes involves transfer of two electrons, whereas this reduction peak has no observable oxidation counter-peak upon cyclic voltammetric back scan. Instead a new oxidation wave appears. This behavior was rationalized as follows. The primary one electron reduction of the parent compound A^+ yields an unstable radical $A^{\backslash}$, which loses rapidly its chlorido ligand, affording a cation-radical $B^{+\backslash}$. Because the reduction potential of $B^{+\backslash}$ can be expected to be more positive compared to A^+ reduction, an immediate one-electron reduction of $B^{+\backslash}$ occurs to give the neutral molecule B (standard ECE mechanism), see Eq. 1. Molecule B resulting from the loss of chlorido ligand is coordinatively unsaturated and can accept one molecule of solvent (acetonitrile or residual water) into its coordination sphere to yield a solvento (aquo)

complex C in its reduced form. During the reverse scan, C is reoxidized, giving rise to an anodic wave in the cyclic voltammogram. The reduction potentials of the first wave do not vary significantly upon substitution of the phenanthroline ligand, whereas they depend very strongly on the type of the arene ligand used. The observed catalytic activity correlates with these reduction potentials thus indicating the decisive role of the η^6-arene ring directly bound to the ruthenium center on the catalytic behavior [7].

1.2. Catalytic properties of Ru(II) complexes

(Arene)Ru(N^N) complexes with N^N being a diamine ligand such as TsDPEN (*N*-(*p*-toluenesulfonyl)-1,2-diphenylethylenediamine) [8] or a diimine ligand as 1,10-phenanthroline (phen) [6,7,9], bipyridine (bpy) [10], bipyrimidine (bpm) [11] or dipyridylamine (dpa) [12] catalyze the transfer hydrogenation of ketones using hydrogen donors such as isopropanol and KOH, the triethylamine/HCOOH azeotropic mixture or even formate in water [13]. In the same vein, several related Ru(II) complexes catalyze the reduction of the ubiquitous cofactors $NAD(P)^+$ into 1,4-NAD(P)H using formate [14,15] or dihydrogen [16].

Regarding the mechanism of transfer hydrogenation, the key species was identified as a ruthenium–hydrido complex [9,10,17,18]. When the hydrogen donor is formate, this metal-hydrido species results from coordination of formate ion to Ru(II) followed by evolution of CO_2 via β-elimination process [10]. This intermediate is able to transfer a hydride to the substrate and when the substrate is a ketone, further addition of a proton provided by the solvent or the N^N ligand affords the alcohol. In the absence of a reducible substrate, the metal hydride reacts with a proton to afford H_2 as shown by GC analysis [10]. Interestingly, hydrido species were also observed after hydrogen transfer from 1,4-NADH to various half-sandwich ruthenium(N^N) complexes (N^N = bpm or phen) as shown by ^{1}H NMR [18]. This

species were in turn able to transfer hydride to lactate to afford pyruvate and thus mimicking the enzyme lactate dehydrogenase.

Formally, generation of ruthenium–hydrido complex requires transfer of one proton and two electrons. Such a process might also occur electrochemically. Indeed, this mechanism has been reported for the isoelectronic $[Cp^*Rh(bpy)(OH_2)]^{2+}$ complex which was shown to behave as an efficient mediator for the indirect electrochemical reduction of NAD^+ [19–22].

1.3. Catalytic properties of Ru(II)/protein conjugate

Artificial metalloenzymes are constructed by incorporation of a synthetic, catalytically competent metallo-cofactor into a protein scaffold [23]. Embedding of (arene)ruthenium(N^N) complexes to the protein hosts (strept)avidin [24–26], papain [1,27–29], carbonic anhydrase [30] or β-lactoglobulin [31] following covalent or supramolecular anchoring strategies afforded artificial metalloenzymes catalyzing (asymmetric) transfer hydrogenation of ketones and reduction of $NAD(P)^+$ in aqueous medium. In addition, covalent anchoring of an $[(arene)Ru(phen)Cl]^+$ complex to papain afforded a bioconjugate displaying catalytic activity on the Lewis acid-catalyzed Diels-Alder reaction between cyclopentadiene and acrolein in water [32]. Also, complex **1** and its papain bioconjugate **1-PAP** were both able to catalyze the reduction of NAD^+ into NADH in the presence of formate [**Erreur ! Signet non défini.**].

In this work we will discuss the electrochemical properties of **1** and its protein conjugate **1-PAP** and their catalytic abilities in connection with the catalytic HER, which is also the simplest reaction catalyzed by many proteins adsorbed on the mercury electrode surface [33,34]. Complex **1** contains one labile chlorido ligand that can be readily replaced in the aqueous solution by a water molecule (hydrolysis of the Ru-Cl bond) to generate active

aquo species [35,36]. On the other hand, hydrolysis can be efficiently suppressed in the presence of excess chloride anions in aqueous solution [**Erreur ! Signet non défini.**,36]. Finally, we will show that phase-sensitive electrochemical techniques can be used to screen the catalytic abilities of an artificial metalloenzyme taking as an example **1-PAP**.

2. Experimental part

2.1. Chemicals

Argon gas (Messer, 99.998 % purity), absolute ethanol (99.8%, molecular biology grade, AppliChem GmbH, Darmstadt, Germany and p.a. Penta, Czech Republic), potassium chloride (Suprapur, Merck) and ferrocene (98% Sigma Aldrich) were used as received. Tetrabutylammonium hexafluorophosphate $TBAPF_6$ (p.a. for electrochemical analysis, ≥ 99% Sigma Aldrich) was dried at 80°C before use. Dimethyl sulfoxide (DMSO, puriss p.a, dried, ≤ 0.02% water, ≥ 99.9% Sigma Aldrich) was further dried with activated molecular sieves (0.3 nm, Lachema, Czech Republic). Ultrapure deionized water with a minimum resistivity of 18.2 MΩ·cm and maximum TOC of 3 ppb was obtained by means of a Milli-Q Integral 5 water purification system (Merck Millipore, France). Compounds **1** and **1-PAP** were synthesized according to a previously published procedure [1,32].

2.2. Experimental methods

DC and AC polarography, AC and cyclic voltammetry (CV) at different scan rates, bulk electrolysis and electrochemical impedance spectroscopy (EIS) were used to characterize molecules **1** and **1-PAP**. The measurements were obtained using either potentiostat PGSTAT30 (Metrohm, Switzerland) or a fast rise-time potentiostat with a lock-in amplifier (model SRS830, Stanford Research, USA). In the latter case the instruments were interfaced to a personal computer via an IEEE-interface card (model PCL-848, PC-Lab, AdvanTech, USA) and a data acquisition card (PCL-818, AdvanTech, USA) using 12-bit precision for

A/D and D/A conversion. Impedance spectra were obtained at 5 mV AC voltage amplitude using the FRA module of PGSTAT30. A three-electrode electrochemical cell was used. A valve–operated hanging mercury drop electrode SMDE2 (Laboratorní přístroje, Prague) was used as working electrode for polarography in the dropping mercury electrode (DME) mode and for CV and impedance measurements in the hanging mercury drop electrode (HMDE) mode. Electrode area in the HMDE mode was 0.0097 cm^2. Mercury pool electrode was used as working electrode for bulk electrolysis. Platinum net served as an auxiliary electrode and reference electrode was Ag|AgCl|1M LiCl separated by a salt bridge from the test solution. Oxygen was removed from the solution directly in the cell by a stream of argon and protective gas layer blanketed the solution throughout the experiment. The ferrocene/ferrocenium redox couple (Fc/Fc^+) was used as an internal reference.

Spectroelectrochemistry was performed using an optically transparent thin-layer cell with CaF_2 optical windows. Working electrode was 5×5 mm^2 Pt gauze (80 mesh) and Ag/AgCl served as the (pseudo)reference electrode. UV-Vis spectra were collected with Agilent 8453 diode-array UV-Vis spectrometer.

2.3. Computational methods

The initial geometry of **1** (cation without a counter ion) was obtained from the crystallographic data of a similar compound with 2,2'-bipyridine ligand [1] by substitution of the ligand for 1,10-phenanthroline. Structure **1** was geometry-optimized using DFT functional B3LYP [37] with the all electron basis set triple-ζ plus polarization function [38]. The relativistic effects were described by Zero Order Regular Approximation (ZORA) including Spin-Orbit coupling [39] and the dispersion correction D3 was used [40]. Cation **1** was gradient-optimized with the neutral doublet electronic state (spin-unrestricted DFT calculation) to obtain the single occupied molecular orbital (SOMO). All quantum chemistry calculations were performed with the program ADF 2017 [41].

3. Results and Discussion

*3.1. Redox properties of compound **1** in DMSO solvent.*

Electrochemical behavior of **1** was studied in DMSO, which represents sufficiently inert solvent that does not compromise the stability of **1** [42]. Representative DC polarogram of **1** in DMSO is shown in Figure 1 and cyclic voltammogram in Figure 2. Red curve in Figure 1 represents DC polarogram of 1,10-phenanthroline (phen), showing redox behavior of this ligand in its free form. Thus polarographic waves at $E_{1/2}$ = –1.721 V and $E_{1/2}$ = –1.908 V of compound **1** can be assigned to reduction of phen ligand in **1** consistently with previously reported studies [3].

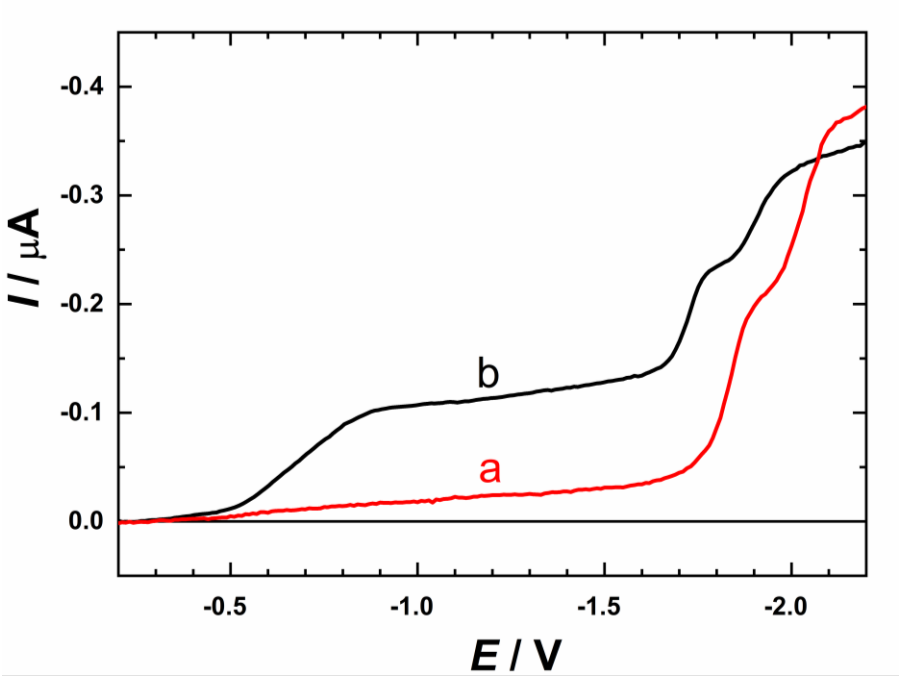

Fig. 1 DC polarography of 1.2×10^{-4} M solution of 1,10-phenanthroline (a) and 4.7×10^{-5} M of **1** (b) in 0.1 M $TBAPF_6$ in DMSO. Drop time was 1.5 s.

Cyclic voltammogram in Figure 2 is the same at switching potential before (less negative) or after (more negative) the phen ligand reduction (see also Figure S1 of the Supporting Information) and the peak current of the first reduction wave (labeled I in Figure 2) depends on the square root of the scan rate.

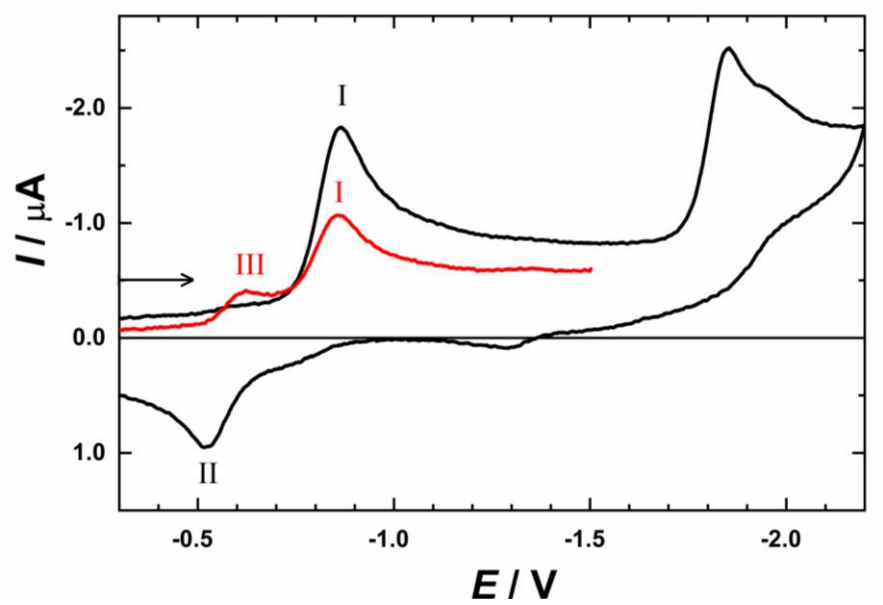

Fig. 2 Cyclic voltammetry of 4.4×10^{-4} M solution of **1** in 0.1 M $TBAPF_6$ and DMSO on glassy carbon electrode at the scan rate 0.5V/s. Arrow indicates the potential scan direction, black line represents first cycle, red line the second cycle. Roman numerals label redox peaks discussed in the text.

Exhaustive bulk electrolysis on mercury pool electrode at potential –0.8V confirmed transfer of two electrons per molecule (n = 2.06). The same number of electrons was obtained by comparison of the cyclic voltammogram of ferrocene with **1** taking the diffusion coefficient of ferrocene as 4.4×10^{-6} cm s^{-1} [43] and assuming the diffusion coefficient of **1** to be 1×10^{-6} cm s^{-1}, see Figure S2 of the Supporting Information (SI). Therefore, we can conclude that the first reduction step of **1** involves transfer of two electrons in DMSO. The reduction peak I has no observable oxidation counter-peak upon cyclic voltammetric back scan, but a new oxidation wave II appears (see Figure 2). This behavior is identical to previously reported results for similar complexes [7,44] where the ECE scheme was suggested to explain this behavior. Thus the ECE mechanism seems to be operative for the reduction of complex **1** as well. As in the previous reports [7,44], a new reduction wave III is observed on the second CV scan (Figure 2, red curve), which can be tentatively assigned to the reduction of a new complex (reaction intermediate) formed after loss of the chlorido ligand and its replacement by the solvent or residual water molecule as ligand.

Assuming that the first electron transfer is the rate-liming step with respect to the overall mechanism we have performed quantum mechanical calculations for **1** after the acceptance of the first electron. Figure 3 shows the gradient optimized structure of **1** in two different views (a,c) and its corresponding SOMO, which characterizes the most probable (de)localization of the first electron within the molecule. Interestingly, the SOMO extends through the phen ligand with significant contribution from ruthenium and chloride atoms (b,d) with a minor contribution from the arene ligand being in accord with the previously proposed ECE process where the chemical reaction involves a subsequent cleavage of the Ru-Cl bond.

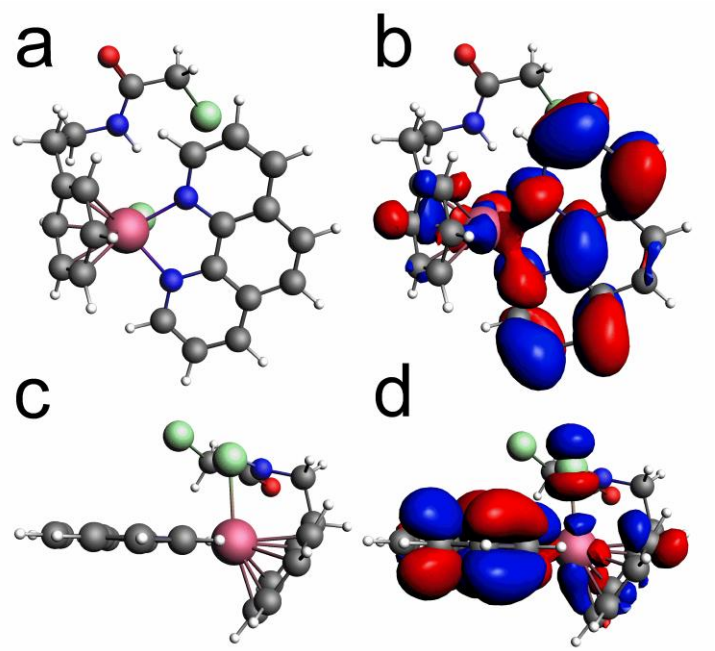

Fig. 3 Optimized chemical structure of **1** (a,c) and its SOMO orbital (b,d). Carbon atoms are shown in grey, nitrogen in blue, oxygen in red, chlorine in green and ruthenium in pink color, respectively.

UV-Vis spectroelectrochemistry was used to characterize spectral changes upon reduction of **1** in DMSO (see Figure S3 of the SI). Consistently with previously proposed ECE mechanism, the appearance of new absorption bands centered at 400 nm, 634 nm and 815 nm points to the processes originating from the charge transfer between the ligand and metal upon reduction. Further assignment of these transitions was not attempted.

*3.2. Redox properties of compound **1** in water solvent.*

Since the aim of this paper is to show that electrochemistry can provide information on the ability of compound **1** and its **1-PAP** conjugate as transfer hydrogenation catalysts in aqueous medium, we have studied first the free compound **1** in 0.1 M KCl aqueous solution. Higher concentration of KCl served not only as the supporting electrolyte but also for stabilization of **1** in water before the electron transfer step, since labile chlorido ligand can be easily replaced by the solvent.

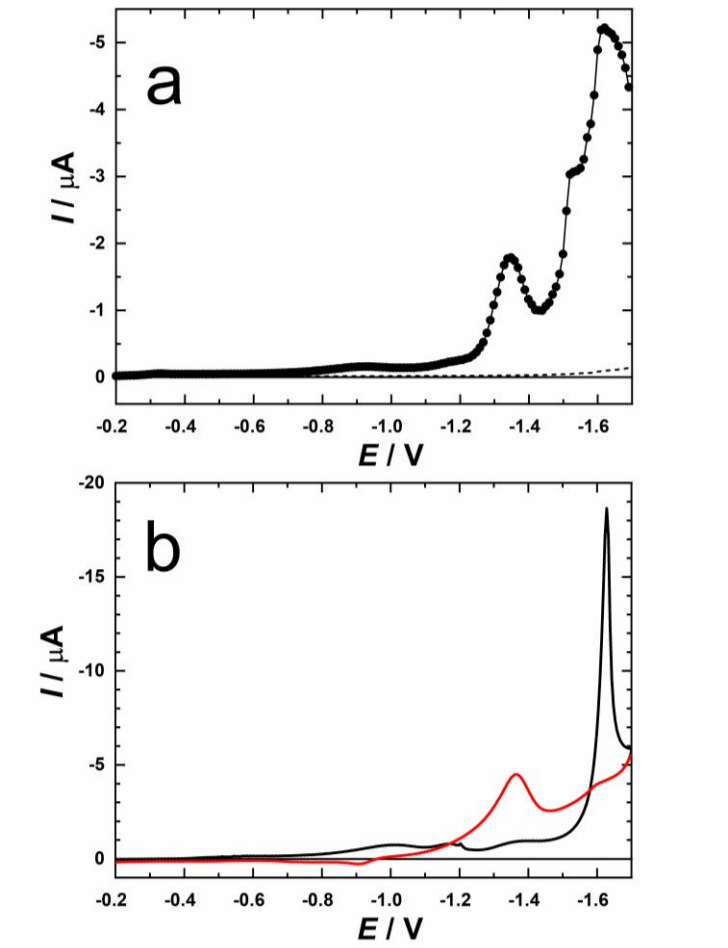

Fig. 4 DC polarography (a) and cyclic voltammetry (b) of 1.8×10^{-5} M **1** in 0.1 M aqueous KCl solution on mercury electrode. DME drop time was 2 seconds (a) and HMDE scan rate was 0.5 V/s (b). Red line indicates the backward scan from –1.7 V to –0.2 V.

Figure 4 shows the DC polarogram (a) and cyclic voltammogram (b) for the reduction of 1.8×10^{-5} M solution of **1** in 0.1 M KCl aqueous solution. Same experiment at ten times

lower concentration of **1** is shown in the Figure S4 of the SI. The most important feature in DC polarogram is the wave at –1.3 V, which corresponds to much higher current than would be expected based on the concentration of **1** and is assigned to the catalytic HER. The same feature is observed in the CV, which additionally shows the current crossing related to the catalytic process [45]. Scheme 1 shows the catalytic cycle for HER catalyzed by **1** assuming the ECE process leading to the neutral complex formation with subsequent formation of the hydrido complex intermediate [7]. Very similar electrochemical behavior (i.e. ECE process with leaving halogenido ligand) has been reported recently for Fe-based HER catalysts [46].

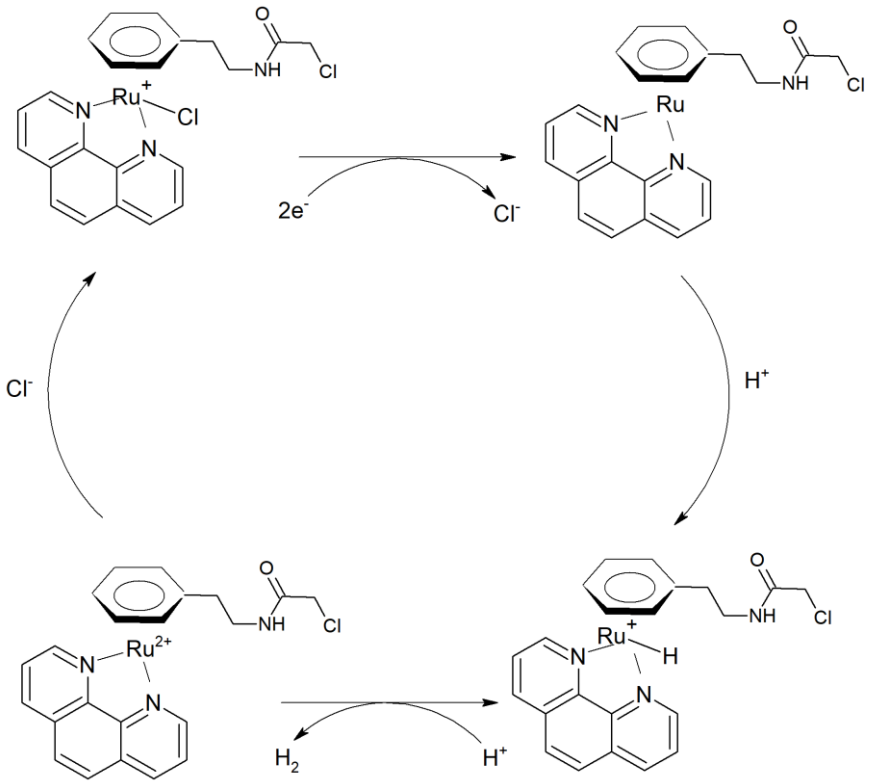

Scheme 1. Schematic presentation of the catalytic cycle for hydrogen evolution reaction in the presence of **1**.

*3.3. AC voltammetry of compounds **1**, **PAP** and **1-PAP** in water.*

Phase-sensitive techniques were used to study HER for three molecules: the organometallic catalyst **1**, papain **PAP** and the artificial metalloprotein **1-PAP**. Figure 5 shows the AC voltammogram for **1** in aqueous KCl solution at the frequency of 16 Hz. Our choice of this frequency is related to the fact that we want to observe kinetics of the HER, which is in general a slow process. Comparison of Figure 5 with that of Figure 4 shows that even at ten

times lower concentration of **1** the catalytic HER manifests itself as two admittance peaks (real *Y*' and imaginary *Y*") at –1.45 V and –1.48 V, respectively. The decrease of *Y*" signal in the AC voltammogram compared to *Y*" in the absence of **1** indicates that **1** adsorbs on the HMDE surface at potentials more negative than –0.3V.

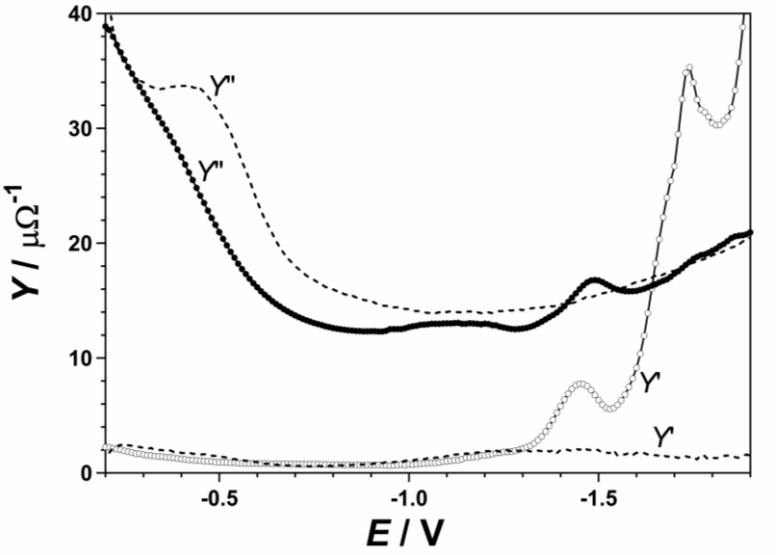

Fig. 5 AC voltammetry of 1.8×10^{-6} M **1** in 0.1 M KCl in water on HMDE. Sine-wave amplitude was ±5mV, frequency 16 Hz and the scan rate 0.0025 V/s. The real and imaginary admittance components are labeled *Y*' and *Y*", respectively. Dotted lines represent aqueous 0.1M KCl supporting electrolyte in the absence of **1**.

Figure 6 shows the AC voltammogram for **PAP** protein. The adsorption of protein on the HMDE electrode is manifested by the decrease of the imaginary admittance component *Y*", whereas two peaks around –1.785 V represent kinetics of the protein-catalyzed HER.

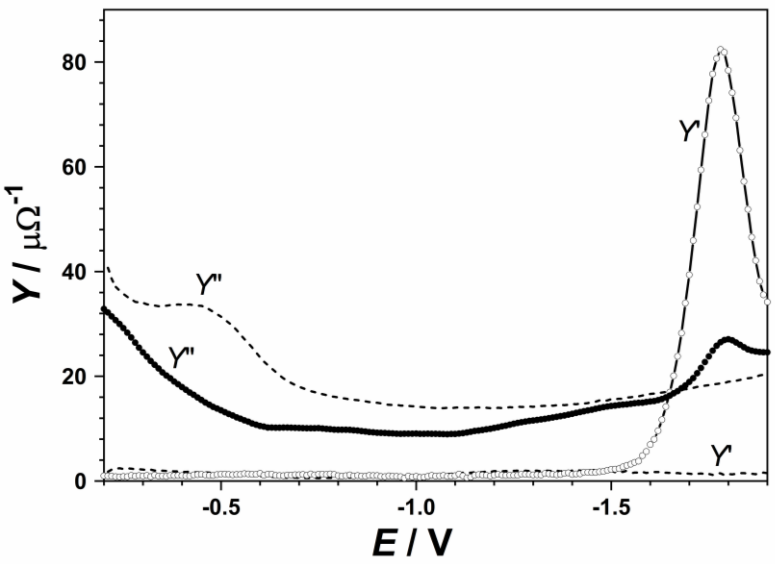

Fig. 6 AC voltammetry of 1×10^{-6} M **PAP** in 0.1 M KCl in water on HMDE. Sine-wave amplitude was ±5mV, frequency 16 Hz and the scan rate 0.0033 V/s. The real and imaginary admittance components are labeled *Y*' and *Y*", respectively. Dotted lines represent aqueous 0.1M KCl supporting electrolyte in the absence of **PAP**.

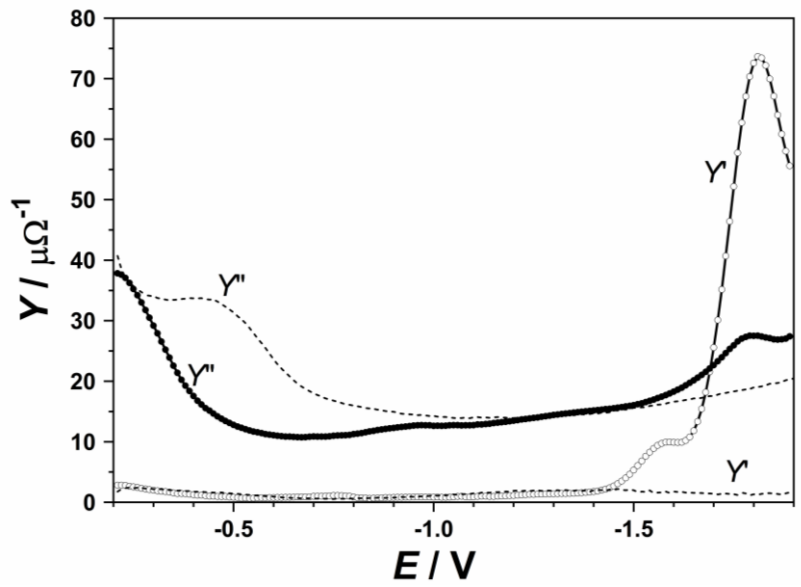

Fig. 7 AC voltammetry of 1×10^{-6} M **1-PAP** in 0.1 M KCl in water on HMDE. Sine-wave amplitude was ±5mV, frequency 16 Hz and the scan rate 0.0033 V/s. The real and imaginary admittance components are labeled *Y*' and *Y*", respectively. Dotted lines represent aqueous 0.1M KCl supporting electrolyte in the absence of **1-PAP**.

Finally, Figure 7 shows the AC voltammogram for **1-PAP** at 16 Hz. By comparison with Figures 5 and 6, it is evident that there are two peaks out of which a more negative one corresponds to HER due to the presence of **PAP** [34] and a more positive one to HER catalyzed by the moiety **1** covalently attached to **PAP** in the **1-PAP** conjugate (evoking parallel to Brdička reaction [47,48]). Interestingly, the *Y*' peak is observed at more negative potentials, which can be interpreted as due to slower HER kinetics.

The AC voltammogram for **1** shown in Fig. 5 and AC voltammogram for **1-PAP** obtained at frequency 1.6 Hz shown in Figure S5 of the SI were used for the determination of HER kinetic rate constants. The appropriate vector analysis of AC voltammograms [49] allows the separation of the measured admittance signal to contributions of the solution resistance, double layer capacitance and the rate parameter $\zeta = Y"_F/(Y'_F - Y"_F)$, where Y'_F and $Y"_F$ represent the real and imaginary components of the faradaic admittance, respectively. Under the assumption that the value of the diffusion coefficient of the redox active species is 1×10^{-5} M cm^2 s^{-1} we obtained the value of $k = 0.023$ cm s^{-1} at E = –1.45 V for HER in the

presence of **1**, whereas the analysis of the AC voltammogram in Figure S5 gave $k = 0.0018$ cm s^{-1} at $E = -1.54$ V for HER in the presence of **1-PAP**. The difference in the electron transfer rate constants was confirmed also by the electrochemical impedance (EIS) studies. Figure 8 compares the EIS spectra obtained at potentials corresponding to the peaks in the AC admittance spectra for HER process catalyzed by compound **1** (Fig. 8a) and the first HER process catalyzed by **1-PAP** (Fig. 8b). Even without fitting the EIS spectra to an appropriate equivalent circuit, one can see that lower charge transfer resistance corresponds to HER observed in the presence of **1**. Indeed, the EIS measurements confirm that the HER catalyzed by **1-PAP** is a slower reduction process compared to HER catalyzed by **1** and proceeds at more negative potentials.

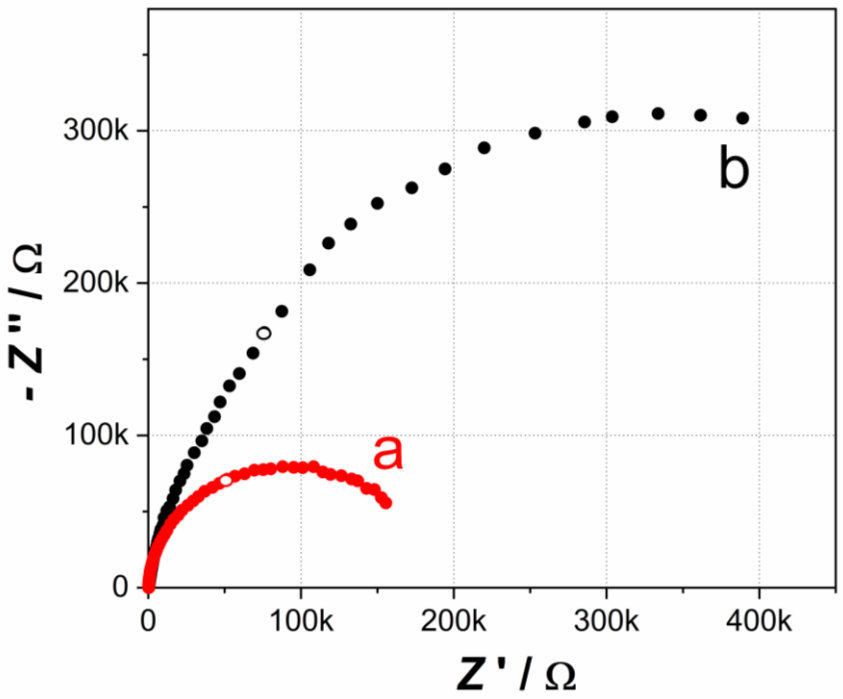

Fig. 8 EIS spectrum for (a) 1.8×10^{-6} M **1** and for (b) 1×10^{-6} M **1-PAP** in 0.1 M aqueous KCl on HMDE. Selected EIS spectra were obtained at potentials within the AC voltammetric peaks of Fig. 5 (E = –1.45V) and Fig. 7 (E = –1.54V). Empty symbols show frequency 10 Hz.

4. Conclusions

The redox mechanism of [(η^6-arene)Ru(1,10-phenanthroline)Cl]Cl (arene = $C_6H_5(CH_2)_2NHCOCH_2Cl$) **1** in DMSO was studied. Combined evidence from DC polarography, cyclic voltammetry, bulk electrolysis, UV-Vis spectroelectrochemistry and

DFT quantum mechanical calculations confirmed the ECE mechanism, where the first electron transfer is followed by dissociation of the labile chlorido ligand and acceptance of a second electron. In accordance with previously suggested catalytic cycles for similar catalytically active organometallic compounds [7,46], the mechanism for HER was suggested. Finally, it was shown that phase-sensitive AC electrochemical methods are well suited for confirmation that the organometallic complex **1** retains its catalytic activity after conjugation to papain, thus making it a fast screening tool for the synthesis of artificial metalloenzymes functioning as hydrogen transfer catalysts. This work showed that **1** is more efficient HER catalyst than **1-PAP**, but its catalytic activity is indeed retained in the **1-PAP** conjugate. These results are in accord with previously reported homogeneous catalytic activity studies of **1-PAP** metalloenzyme [32]. Further analysis of different types of metalloenzymes is needed to make this demonstration an efficient screening tool.

Acknowledgement

Financial support by the Czech Science Foundation (18-04682S), Czech Academy of Sciences (RVO: 61388955), the Ministry of Education of the Czech Republic (Barrande project 8J18FR002), the French Ministries of Foreign Affairs (MAE) and Higher Education and Research (MESR) (PHC Barrande, 2018 project No. 34012SC) is gratefully acknowledged.

Appendix A. **Supplementary data**

References

[1] P. Haquette, B. Talbi, S. Canaguier, S. Dagorne, C. Fosse, A. Martel, G. Jaouen, M. Salmain, Functionalized cationic (η^6-arene)ruthenium(II) complexes for site-specific and covalent anchoring to papain from papaya latex. Synthesis, X-ray structures and reactivity studies, Tetrahedron Lett. 49 (2008) 4670–4673.

[2] B. K. Ghosh, A. Chakravorty, Electrochemical studies of ruthenium compounds. Part I. Ligand oxidation levels, Coord. Chem. Rev. 95 (1989) 239–294.
[3] N. E. Tokel-Takvoryan, R. E. Hemingway, A. J. Bard, Electrogenerated Chemiluminescence. XIII. Electrochemical and Electrogenerated Chemiluminescence Studies of Ruthenium Chelates, J. Am. Chem. Soc. 95 (1973) 6582–6589.
[4] N. K. Shee, Sh. G. Patra, M. G. B. Drew, L. Lu, E. Zangrando, D. Datta, Electrochemical behaviour of tris(1,10-phenanthroline)ruthenium(II) at a surface modified electrode. Electrocatalytic reduction of dioxygen, Inorg. Chim. Acta 466 (2017) 349–357.
[5] H. Yi, A. Jutand, A. Lei, Evidence for the interaction between tBuOK and 1,10-phenanthroline to form the 1,10-phenanthroline radical anion: a key step for the activation of aryl bromides by electron transfer, Chem. Commun. 51 (2015) 545–548.
[6] J. Canivet, G. Süss-Fink, P. Štěpnička, Water-Soluble Phenanthroline Complexes of Rhodium, Iridium and Ruthenium for the Regeneration of NADH in the Enzymatic Reduction of Ketones, Eur. J. Inorg. Chem. (2007) 4736–4742.
[7] P. Štěpnička, J. Ludvík, J. Canivet, G. Süss-Fink, Relating catalytic activity and electrochemical properties: The case of arene–ruthenium phenanthroline complexes catalytically active in transfer hydrogenation, Inorg. Chim. Acta 359 (2006) 2369–2374.
[8] R. Noyori, M. Yamakawa, S. Hashiguchi, Metal-Ligand Bifunctional Catalysis: A Nonclassical Mechanism for Asymmetric Hydrogen Transfer between Alcohols and Carbonyl Compounds, J. Org. Chem. 66 (2001) 7931–7944.
[9] J. Canivet, L. Karmazin-Brelot, G. Süss-Fink, Cationic arene ruthenium complexes containing chelating 1,10-phenanthroline ligands, J. Organomet. Chem. 690 (2005) 3202–3211.
[10] S. Ogo, T. Abura, Y. Watanabe, pH-Dependent Transfer Hydrogenation of Ketones with HCOONa as a Hydrogen Donor Promoted by (η^6-C_6Me_6)Ru Complexes, Organometallics 21 (2002) 2964–2969.
[11] P. Govindaswamy, J. Canivet, B. Therrien, G. Süss-Fink, P. Štěpnička, J. Ludvík, Mono and dinuclear rhodium, iridium and ruthenium complexes containing chelating 2,2'-bipyrimidine ligands: Synthesis, molecular structure, electrochemistry and catalytic properties, J. Organomet. Chem. 692 (2007) 3664–3675.
[12] Ch. Romain, S. Gaillard, M. K. Elmkaddem, L. Toupet, C. Fischmeister, Ch. M. Thomas, J.-L. Renaud, New Dipyridylamine Ruthenium Complexes for Transfer Hydrogenation of Aryl Ketones in Water, Organometallics 29 (2010) 1992–1995.
[13] A. Robertson, T. Matsumoto, S. Ogo, The development of aqueous transfer hydrogenation catalysts, Dalton Trans. 40 (2011) 10304–10310.
[14] Y. K. Yan, M. Melchart, A. Habtemariam, A. F. A. Peacock, P. J. Sadler, Catalysis of regioselective reduction of NAD^+ by ruthenium(II) arene complexes under biologically relevant conditions, J. Biol. Inorg. Chem. 11 (2006) 483–488.
[15] J. J. Soldevila-Barreda, P. C. A. Bruijnincx, A. Habtemariam, G. J. Clarkson, R. J. Deeth, P. J. Sadler, Improved Catalytic Activity of Ruthenium−Arene Complexes in the Reduction of NAD^+, Organometallics 31 (2012) 5958–5967.
[16] P. S. Wagenknecht, J. M. Penney, R. T. Hembre, Transition-Metal-Catalyzed Regeneration of Nicotinamide Coenzymes with Hydrogen, Organometallics 22 (2003) 1180–1182.
[17] R. R. Dykeman, K. L. Luska, M. E. Thibault, M. D. Jones, M. Schlaf, M. Khanfar, N. J. Taylor, J. F. Britten, L. Harrington, Catalytic deoxygenation of terminal-diols under acidic aqueous conditions by the ruthenium complexes [(η^6-arene)Ru(X)(N∩N)](OTf)$_n$, X = H_2O, H, η_6-arene = *p*-Me-^{i}Pr-C_6H_4, C_6Me_6, N∩N = bipy, phen, 6,6'-diamino-bipy, 2,9-diamino-

phen, *n*=1, 2). Influence of the *ortho*-amine substituents on catalytic activity, J. Mol. Catal. A: Chem. 277 (2007) 233–251.
[18] S. Betanzos-Lara, Z. Liu, A. Habtemariam, A. M. Pizarro, B. Qamar, P. J. Sadler, Organometallic Ruthenium and Iridium Transfer-Hydrogenation Catalysts Using Coenzyme NADH as a Cofactor, Angew. Chem. Int. Ed. 51 (2012) 3897–3900.
[19] R. Ruppert, S. Herrmann, E. Steckhan, Efficient Indirect Electrochemical In-situ Rregeneration of NADH: Electrochemically Driven Enzymatic Reduction of Pyruvate Catalyzed by D-LDB, Tetrahedron Lett. 28 (1987) 6583–6586.
[20] R. Ruppert, S. Herrmann, E. Steckhan, Very Efficient Reduction of $NAD(P)^+$ with Formate catalysed by Cationic Rhodium Complexes, J. Chem. Soc., Chem. Commun. (1988) 1150–1151.
[21] E. Steckhan, S. Herrmann, R. Ruppert, J. Thommes, Ch. Wandrey, Continuous Generation of NADH from NAD^+ and Formate Using a Homogeneous Catalyst with Enhanced Molecular Weight in a Membrane Reactor, Angew. Chem. Int. Ed. 29 (1990) 388–390.
[22] E. Steckhan, S. Herrmann, R. Ruppert, E. Dietz, M. Frede, E. Spika, Analytical study of a series of substituted (2,2'-bipyridyl)(pentamethylcyclopentadienyl)rhodium and –iridium complexes with regard to their effectiveness as redox catalysts forthe indirect electrochemical and chemical reduction of $NAD(P)^+$, Organometallics 10 (1991) 1568–1577.
[23] F. Schwizer, Y. Okamoto, T. Heinisch, Y. Gu, M. M. Pellizzoni, V. Lebrun, R. Reuter, V. Köhler, J. C. Lewis, T. R. Ward, Artificial Metalloenzymes: Reaction Scope and Optimization Strategies, Chem. Rev. 118 (2018) 142–231.
[24] C. Letondor, N. Humbert, T. R. Ward, Artificial metalloenzymes based on biotin-avidin technology for the enantioselective reduction of ketones by transfer hydrogenation, Proc. Natl Acad. Sci. USA 102 (2005) 4683–4687.
[25] M. Creus, A. Pordea, T. Rossel, A. Sardo, C. Letondor, A. Ivanova, I. Le Trong, R. E. Stenkamp, T. R. Ward, X-Ray Structure and Designed Evolution of an Artificial Transfer Hydrogenase, Angew. Chem. Int. Ed. 47 (2008) 1400–1404.
[26] A. Pordea, M. Creus, C. Letondor, A. Ivanova, T. R. Ward, Improving the enantioselectivity of artificial transfer hydrogenases based on the biotin–streptavidin technology by combinations of point mutations, Inorg. Chim. Acta 363 (2010) 601–604.
[27] P. Haquette, B. Dumat, B. Talbi, S. Arbabi, J.-L. Renaud, G. Jaouen, M. Salmain, Synthesis of N-functionalized 2,2'-dipyridylamine ligands, complexation to ruthenium (II) and anchoring of complexes to papain from papaya latex, J. Organomet. Chem. 694 (2009) 937–941.
[28] P. Haquette, J. Jacques, S. Dagorne, C. Fosse, M. Salmain, Synthesis, Characterization and Luminescence Properties of Dipyridin-2-ylamine Ligands and Their Bis(2,2'-bipyridyl)ruthenium(II) Complexes and Labelling Studies of Papain from *Carica papaya*, Eur. J. Inorg. Chem. (2010) 5087–5095.
[29] N. Madern, B. Talbi, M. Salmain, Aqueous phase transfer hydrogenation of aryl ketones catalysed by achiral ruthenium(II) and rhodium(III) complexes and their papain conjugates, Appl. Organometal. Chem. 27 (2013) 6–12.
[30] F. W. Monnard, T. Heinisch, E. S. Nogueira, T. Schirmer, T. R. Ward, Human Carbonic Anhydrase II as a host for piano-stool complexes bearing a sulfonamide anchor, Chem. Commun. 47 (2011) 8238–8240.
[31] A. Chevalley, M. V. Cherrier, J. C. Fontecilla-Camps, M. Ghasemia, M. Salmain, Artificial metalloenzymes derived from bovine β-lactoglobulin for the asymmetric transfer

hydrogenation of an aryl ketone – synthesis, characterization and catalytic activity, Dalton Trans. 43 (2014) 5482–5489.
[32] B. Talbi, P. Haquette, A. Martel, F. de Montigny, C. Fosse, S. Cordier, Th. Roisnel, G. Jaouen, M. Salmain, (η^6-Arene) ruthenium(II) complexes and metallo-papain hybrid as Lewis acid catalysts of Diels–Alder reaction in water, Dalton Trans. 39 (2010) 5605–5607.
[33] M. Heyrovský, Early Polarographic Studies on Proteins, Electroanalysis 16 (2004) 1067–1073.
[34] Th. Doneux, V. Ostatná, E. Paleček, On the mechanism of hydrogen evolution catalysis by proteins: A case study with bovine serum albumin, Electrochim. Acta 56 (2011) 9337–9343.
[35] F. Wang, A. Habtemariam, E. P. L. van der Geer, R. Fernández, M. Melchart, R. J. Deeth, R. Aird, S. Guichard, F. P. A. Fabbiani, P. Lozano-Casal, I. D. H. Oswald, D. I. Jodrell, S. Parsons, P. J. Sadler, Controlling ligand substitution reactions of organometallic complexes: Tuning cancer cell cytotoxicity, Proc. Natl. Acad. Sci. USA 102 (2005) 18269–18274.
[36] A. M. Pizarro, A. Habtemariam, P. J. Sadler, Activation Mechanisms for Organometallic Anticancer Complexes, Top. Organomet. Chem. 32 (2010) 21–56.
[37] P. J. Stephens, F. J. Devlin, C. F. Chabalowski, M. J. Frisch, Ab Initio Calculation of Vibrational Absorption and Circular Dichroism Spectra Using Density Functional Force Fields, J. Phys. Chem. 98 (1994) 11623–11627.
[38] E. van Lenthe, E. J. Baerends, Optimized Slater-type basis sets for the elements 1-118, J. Comput. Chem. 24 (2003) 1142–1156.
[39] E. van Lenthe, E. J. Baerends, J. G. Snijders, Relativistic regular two-component Hamiltonians, J. Chem. Phys. 99 (1993) 4597–4610.
[40] S. Grimme, J. Anthony, S. Ehrlich, H. Krieg, A consistent and accurate *ab initio* parametrization of density functional dispersion correction (DFT-D) for the 94 elements H-Pu, J. Chem. Phys. 132 (2010) 154104–154105.
[41] G. te Velde, F. M. Bickelhaupt, E. J. Baerends, C. Fonseca Guerra, S. J. A. van Gisbergen, J. G. Snijders, T. Ziegler, Chemistry with ADF, J. Comput. Chem. 22 (2001) 931–967.
[42] L. Biancalana, L. K. Batchelor, T. Funaioli, S. Zacchini, M. Bortoluzzi, G. Pampaloni, P. J. Dyson, F. Marchetti, α−Diimines as Versatile, Derivatizable Ligands in Ruthenium(II) p−Cymene Anticancer Complexes, Inorg. Chem. 57 (2018) 6669–6685.
[43] N. G. Tsierkezos, Cyclic Voltammetric Studies of Ferrocene in Nonaqueous Solvents in the Temperature Range from 248.15 to 298.15 K, J. Solution Chem. 36 (2007) 289–302.
[44] H. tom Dieck, W. Kollvitz, I. Kleinwachter, Ruthenium Complexes with Diazadienes. 4.[1] Arene Diazadiene Ruthenium(II) Complexes [(η^6-Arene)(RN=CR'—CR'=NR)Ru(L)]$^{n+}$ (n = 1, L = Cl, I, Alkyl; n = 2, L = MeCN, η^2-C_2H_4) and Arene Diazadiene Ruthenium(0), Organometallics 5 (1986) 1449–1457.
[45] V. Fourmond, Ch. Léger, Modelling the voltammetry of adsorbed enzymes and molecular catalysts, Current Opinion in Electrochemistry 1 (2017) 110–120.
[46] E. B. Hemming, B. Chan, P. Turner, L. Corcilius, J. R. Price, M. G. Gardiner, A. F. Masters, T. Maschmeyer, [Fe(C_5Ar_5)$(CO)_2$Br] complexes as hydrogenase mimics for the catalytic hydrogen evolution reaction, Appl. Cat. B: Environmental 223 (2018) 234–241.
[47] R. Brdička, M. Březina, V. Kalous, Polarography of Proteins and its Analytical Aspects, Talanta 12 (1965) 1149–1162.
[48] B. Raspor, Elucidation of the mechanism of the Brdička reaction, J. Electroanal. Chem. 503 (2001) 159–162.

[49] V. Brabec, D. Walz, G. Milazzo (Eds.) Experimental techniques in bioelectrochemistry, (Bioelectrochemistry, Vol. 3), Birkhäuser, Basel, 1996.